ACS chemical biology

Reviews

Cite This: ACS Chem. Biol. 2018, 13, 1810−1823

Enzyme-Activated Fluorogenic Probes for Live-Cell and *in Vivo* Imaging

Wen Chyan and Ronald T. Raines*

Department of Chemistry, Massachusetts Institute of Technology, Cambridge, Massachusetts 02139, United States

ABSTRACT: Fluorogenic probes, small-molecule sensors that unmask brilliant fluorescence upon exposure to specific stimuli, are powerful tools for chemical biology. Those probes that respond to enzymatic catalysis illuminate the complex dynamics of biological processes at a level of spatiotemporal detail and sensitivity unmatched by other techniques. Here, we review recent advances in enzyme-activated fluorogenic probes for biological imaging. We organize our survey by enzyme classification, with emphasis on fluorophore masking strategies, modes of enzymatic activation, and the breadth of current and future applications. Key challenges such as probe selectivity and spectroscopic requirements are described alongside therapeutic, diagnostic, and theranostic opportunities.

Fluorogenic probes are latent fluorophores that reveal their signal in response to environmental changes, interactions with analytes, or specific chemical reactions.[1] Fluorogenic probes are prepared by chemically modulating the fluorescence of a parent fluorophore, rendering it nonfluorescent until activation by a specific triggering event. Because of their high sensitivity and ability to monitor diverse events selectively, fluorogenic probes are important components in the toolkit of chemical biology.[2−4]

Enzyme-activated fluorogenic probes, which invoke enzymatic catalysis to trigger the generation of fluorescence, provide a versatile platform for monitoring biological processes in live cells and *in vivo*. Early enzyme-activated probes were based on xanthene dye scaffolds and detected galactosidases, phosphatases, lipases, and esterases.[5−8] Later, rudimentary live-cell imaging was demonstrated with cell-permeable probes,[9] leading to modern probe applications, including cell-viability assays,[10] diagnostic tests,[11] and immunoassay technologies such as enzyme-linked immunosorbent assays (ELISAs).[12] Innovations in probe design continue to drive the development of companion techniques and applications.

The two overarching themes for fluorogenic probe design and applications are the spectroscopic properties of the parent fluorophore and the method employed to mask its fluorescence. Key properties of the parent fluorophore include brightness (which is the product of quantum yield and extinction coefficient), wavelengths and shapes of both excitation and emission peaks, effects of pH on fluorescence, and resistance to photobleaching. Recent trends in fluorophore scaffolds include the reduction of phototoxicity and autofluorescence background with far-red,[13] near-infrared,[14] and two-photon excited probes[15] and the fine-tuning of spectroscopic properties and brightness.[16,17] Whereas parent fluorophore properties determine the postactivation performance of a probe, the fluorescence masking strategy governs its enzymic target and responsiveness. Accordingly, we focus this review on enzyme-catalyzed unmasking strategies that have been used for imaging in live cells and *in vivo*. We also constrain our survey to the past five years and abstain from extensive discussion of parent fluorophore chemistry and spectroscopic properties covered elsewhere.[3,16−19]

PROBE DESIGN

Optimal fluorescence masking methods are chemically stable, respond selectively to the desired event, and completely eliminate fluorescence and absorption at the excitation wavelength via quenching, masking groups, or other chemical modifications. Three main methods for modulating fluorescence in enzyme-activated fluorogenic probes are depicted in Scheme 1. Although masking groups to block constitutive fluorescence (Scheme 1A,B) are employed frequently, quenching strategies based on Förster resonance energy transfer (FRET) or photoinduced electron transfer (PET) effects can provide high modularity and, in some cases, ratiometric imaging (Scheme 1C). Other common themes for enzyme activation include fluorophore precipitation and autoimmolative linkers that can improve probe stability and performance.[20] The two most frequently encountered autoimmolative motifs, elimination and acyl transfer, are used to release a fluorophore payload rapidly and spontaneously (Scheme 2).

Special Issue: Sensors

Received: April 21, 2018
Accepted: June 20, 2018
Published: June 20, 2018

DOI: 10.1021/acschembio.8b00371
ACS Chem. Biol. 2018, 13, 1810−1823

Scheme 1. Common Fluorescence Modulation Methods in Enzyme-Activated Fluorogenic Probes, with Examples for Each Method, (A) Enzymatic Cleavage of Blocking Groups, (B) Enzymatic Conversion of Blocking Groups into Other Functional Groups, and (C) Enzymatic Release of FRET or PET Quenchers

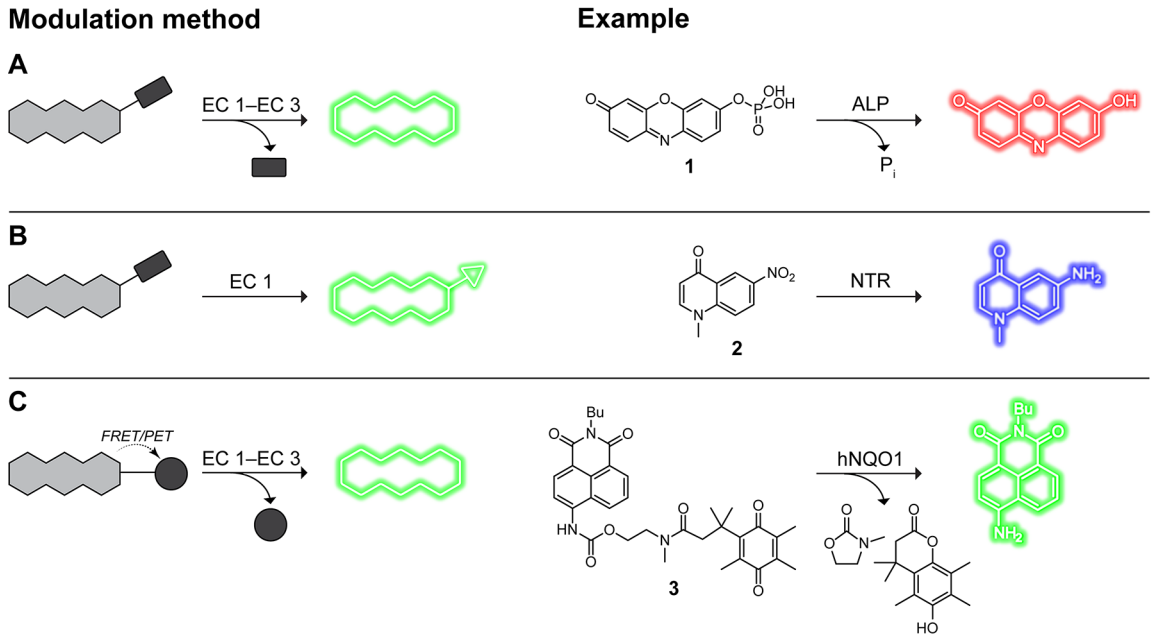

Scheme 2. Representative Examples of Two Predominant Mechanisms of Activation in Autoimmolative Linkers, (A) Elimination and (B) Acyl Transfer[a]

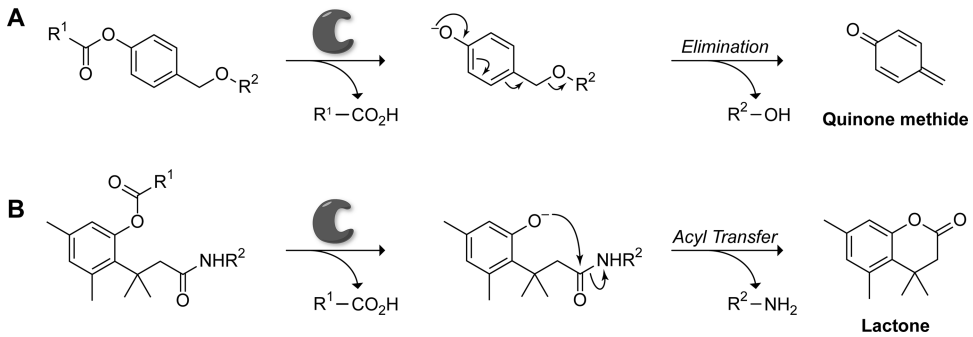

[a]Enzymatic catalysis releases a masking group (R^1-CO_2H). Then, elimination to form a quinone methide (A)[27] or acyl transfer driven by the action of a trimethyl lock (B)[25] rapidly releases a fluorophore (R^2-OH or R^2-NH_2).

Because the intracellular space is a dense heterogeneous mixture of molecules, organelles, and other subcellular structures, the complexity of biological systems is more faithfully represented by live-cell and *in vivo* models than by fixed-cell or isolated enzyme experiments.[21,22] The rich trove of dynamic cellular processes that can be studied in live cells is not accessible to fixed-cell imaging or other disruptive methods. As a result, probe technologies developed using live-cell and *in vivo* models translate more readily to therapeutic, diagnostic, and clinical applications.[23,24] Indeed, fluorogenic probes and masking groups are often inspired by prodrug and inhibitor design strategies.[15,25,26]

Operating in the crowded cellular environment poses additional challenges to the design of enzyme-activated probes for biological imaging applications. Constraints include optimizing the rates and specificities of enzymatic activation, directing probe uptake and localization, enhancing probe stability, and minimizing toxicity. Probe stability, enzyme specificity, and rate of activation are heavily influenced by the method of fluorescence modulation. In probes that employ a masking or blocking strategy (Scheme 1A,B), covalently attached groups serve as both the enzyme-responsive moiety and fluorescence masking group. In contrast, probes utilizing quenching techniques require the addition of a separate enzyme-responsive group (Scheme 1C). Conversely, the modularity of masking and enzyme-responsive groups provides a convenient method of adapting fluorophore scaffolds to target different enzymes.

■ ENZYME TARGETS

To frame our review, we employ the enzyme classification system established by the International Union of Biochemistry and Molecular Biology (IUBMB). This system relies on the type of reaction catalyzed by the enzyme: oxidoreductases (EC 1), transferases (EC 2), hydrolases (EC 3), lyases (EC 4), isomerases (EC 5), and ligases (EC 6).[28] The majority of enzyme-activated probes target enzymes in classes EC 1–EC 3. The sparsity of probes targeting EC 4–EC 6 can be attributed,

DOI: 10.1021/acschembio.8b00371
ACS Chem. Biol. 2018, 13, 1810–1823

Table 1. Targeted Enzymes and Imaging Applications of Enzyme-Activated Probes

EC	enzymes	applications	tested cell lines and tissues	model organisms	probes
1.4	monoamine oxidase	Parkinson's disease diagnosis, inhibitor screening	Hep-G2, SH-SY5Y	*Drosophila melanogaster*, mice	**4**, **5**
1.6	NAD(P)H:quinone oxidoreductase	rapid cancer-cell screening, tissue resection	A549, HT29, H446, H596, OVCAR-3	–	**3**, **6**, **7**
	nitroreductases	antibiotic-resistant pathogen identification	–	*Enterococcus faecium*, *Staphylococcus aureus*, *Klebsiella pneumoniae*, *Acinetobacter baumannii*	**8**
		organelle-specific imaging in hypoxic tumor cells	A549, HEK293, HeLa, HTC116, liver	–	**2**, **9**–**14**, **16**
		selective mitochondrial imaging and drug delivery	A549, BT474, DU145, WI38	–	**15**
1.7	azoreductase	orthogonal reporter system	A549, HEK293T, HeLa, NIH-3T3	–	**17**
1.8	thioredoxin reductase	thioredoxin reductase-selective imaging in live cells	Hep-G2	–	**18**
1.14	ALKBH3	prostate cancer-targeted therapy and inhibitor screening	B16, HeLa	zebrafish	**19**
	tyrosinase	vitiligo and Parkinson's disease diagnosis	PC3, U2OS	–	**20**
2.3	γ-glutamyltranspeptidase	intraoperative fluorescence imaging	SHIN3, SKOV3, colon	–	**21**, **22**
	mycolyltransferases	study of mycobacterial-cell growth and division	–	*Mycobacterium smegmatis*, *Corynebacterium glutamicum*	**23**
2.5	glutathione *S*-transferase	isoform-selective glutathione transferase imaging	HL60	–	**24**
2.7	Bruton's tyrosine kinase	single-step selective kinase imaging	Jurkat, Namalwa	–	**25**
3.1.1	carboxylesterases	super-resolution study of enzymatic activity	CHO, *Drosophila* S2, HEK293, HeLa, WBF344, neurons, brain	–	**26**
		orthogonal enzyme–probe pair, improved probe properties	HeLa	–	**27**, **28**
		theranostic agents	hiPSC neurons, neuro-2A	–	**29**
		pathogen profiling and detection	–	*Mycobacterium tuberculosis*	**30**
		prodrug activation and multicolor imaging of ER esterases	HeLa, HT1080, SK-N-SH	–	**31**
		study of endocytic processes in cancer cells	HeLa, HTB125, HTB126	–	**32**
3.1.2	acyl-protein thioesterase (APT)	study of cellular responses to lipid stress, ratiometric imaging, and visualization of mitochondrial APT	A549, HeLa, HEK293T, Hep-G2, MCF-7	human colon organoids	**33**–**35**
3.1.3	alkaline phosphatase (ALP)	monitoring excreted phosphatases, near-infrared imaging of ALP	HeLa, Hep-G2, U-2OS tissue, Saos-2 tissue	*D. melanogaster*, mice	**36**, **37**
	protein tyrosine phosphatase (PTP)	two-photon visualization of PTP	HEK293, HeLa, Hep-G2	*Staphylococcus saprophyticus*, *E. faecalis*, *A. baumannii*, *S. aureus*	**1**, **38**
3.2	β-galactosidase	tracking of cell senescence, quantification of cytosolic delivery	C6, HeLa, SK-MEL-103	mice	**39**, **40**
	glucocerebrosidase	study of lysosomal storage disorders	fibroblasts	–	**41**
	β-glucuronidase	deep-tissue tumor imaging	–	mice	**42**
3.4	β-alanyl aminopeptidase	pathogen detection	–	*Pseudomonas aeruginosa*, *Serratia marcescens*, *Burkholderia cepacia*	**43**
	hepsin matriptase	prostate cancer imaging	DU145, LNCaP, PC3, PrEC	mice	**44**
	cathepsin B and S	deep-tissue tumor imaging of lysosomal cathepsins	HEK293, HeLa, KB, MCF-7, MDA-MB-231, NIH-3T3, dendritic cells, U87	mice	**45**–**47**
	caspase-3	visualization of pre-apoptotic enzymatic activity	HeLa	–	**48**
	ER aminopeptidase	two-photon ER-targeted deep-tissue redox imaging	HeLa	–	**49**
3.5	β-lactamases	detection and labeling of antibiotic-resistant pathogens	–	*Escherichia coli*, *M. tuberculosis*	**50**, **51**

at least partially, to the inaccessibility of fluorescence modulation mechanisms for reactions catalyzed by these enzymes. Probes targeting oxidoreductases in EC 1 employ the widest variety of fluorescence modulation strategies, whereas probes targeting EC 2 and EC 3 enzymes primarily rely on FRET/PET quenching or masking groups (Scheme 1A,C). Although probes for the three main enzyme classes, EC 1–EC 3, have existed for several decades, recent advances in probe chemistry and design have rejuvenated the field with methods for tuning spectroscopic properties and enzyme specificity.[15,17,26]

Below, we describe advances in enzyme-activated probes for biological imaging, organized by enzyme type. Each section contains descriptions of targeted enzyme classes or subclasses, modes of enzyme activation, and applications to live-cell and *in vivo* imaging. A summary of enzymes, probes, applications, and model cell lines and organisms can be found in Table 1.

OXIDOREDUCTASES (EC 1)

Oxidoreductases make up a highly diverse class of enzymes that oxidize or reduce a wide variety of substrates, often with cofactors NAD(P)H and flavin mononucleotide (FMN).

DOI: 10.1021/acschembio.8b00371
ACS Chem. Biol. 2018, 13, 1810–1823

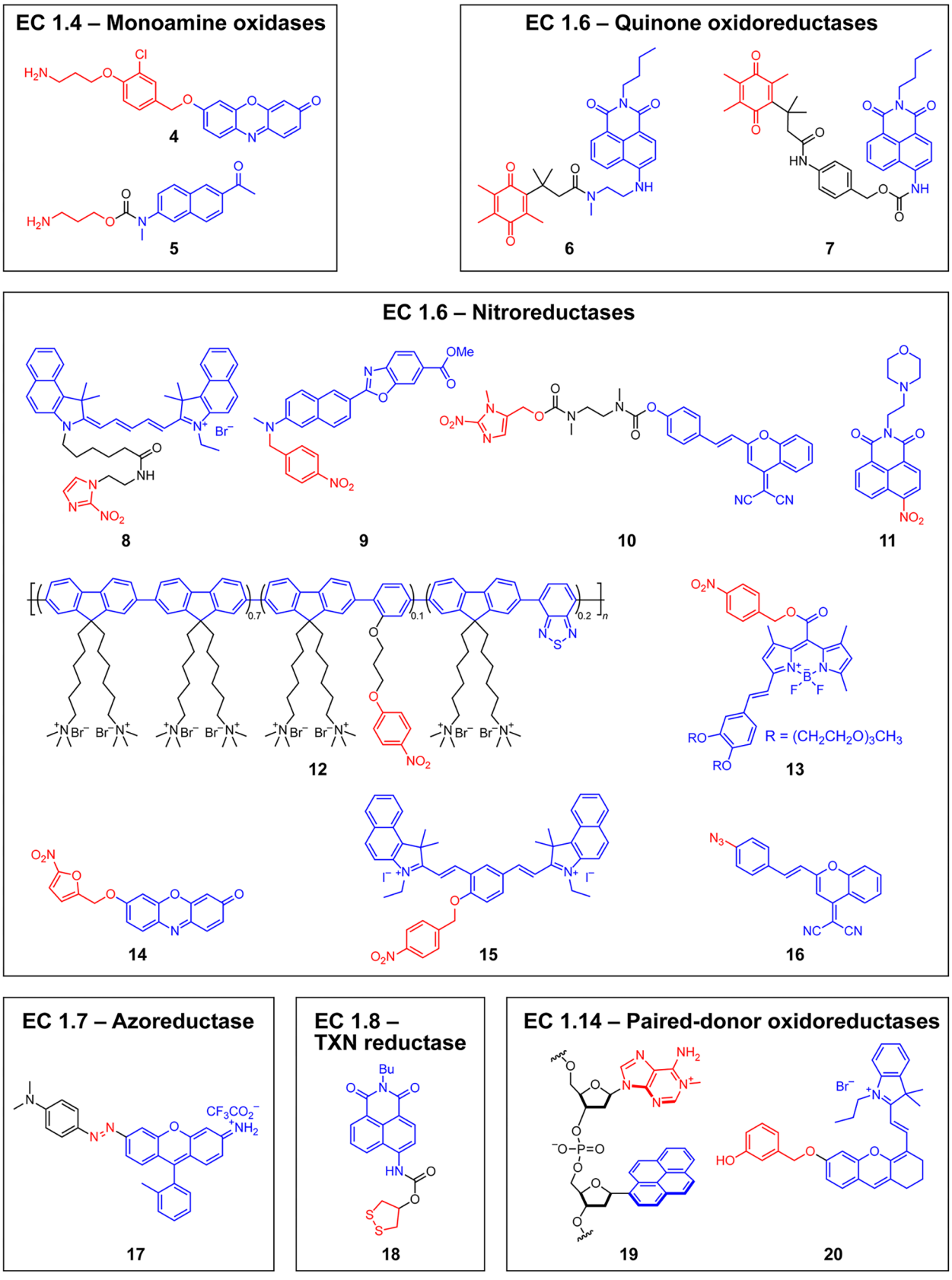

Figure 1. Structures of probes activated by oxidoreductase enzymes EC 1.4−1.6, EC 1.8, and EC 1.14. Enzyme-reactive moieties (red) and fluorophore scaffolds (blue) are highlighted.

DOI: 10.1021/acschembio.8b00371
ACS Chem. Biol. 2018, 13, 1810−1823

These enzymes are classified further as oxidases or dehydrogenases depending on the nature of the redox reaction and the final electron acceptor. Oxidases transfer electrons to molecular oxygen as the acceptor, whereas dehydrogenases remove hydrogens from a donor in an NAD^+- or FAD-dependent manner. Of the 22 different types of oxidoreductases, most fluorogenic probes target those classes relevant to pathogen detection and tumor imaging, diagnosis, and treatment. Key foci of recent work involve creating tools to investigate cancer biomarkers, tumor-cell hypoxia, and neurodegenerative diseases.

Oxidoreductases That Act on the CH-NH_2 Group of Donors (EC 1.4). Oxidoreductases of subclass EC 1.4 include enzymes such as monoamine oxidase (MAO) that are associated with the outer mitochondrial membrane and catalyze the oxidative deamination of amines to aldehydes (Figure 1).[29] Although both MAO-A and MAO-B isoforms are bound to mitochondria and abundant in the brain, they are differentially localized at a cellular and tissue level and have distinct substrate preferences. Isoforms MAO-A and MAO-B are targets for the treatment of Parkinson's disease, as both MAO enzymes are important for maintaining hormone and neurotransmitter homeostasis.[29] Two-photon excited probes **4** and **5** were developed recently to monitor MAO-A and MAO-B activity selectively in deep-tissue imaging.[15,26] Probe **4** is based on a resorufin scaffold with a linker connecting the fluorophore and propylamine enzyme-reactive moiety. MAO-A specificity is conferred by the *ortho*-halogenated linker, which is inspired by the MAO-A inhibitor clorgiline and also serves as an autoimmolative linker that undergoes elimination to release a quinone methide. Probe **5** is based on the acedan scaffold and derives its selectivity for MAO-B from a carbamate linker moiety, inspired by the MAO-B inhibitor pargyline and optimized by *in silico* molecular docking. Probes **4** and **5** demonstrate the utility of drug- and inhibitor-inspired probe design and enable selective imaging of MAO-A and MAO-B in live cells as well as in *Drosophila* and mouse models of Parkinson's disease.

Oxidoreductases Acting on NADH or NADPH (EC 1.6). The most frequently encountered enzymes in EC 1.6 are quinone oxidoreductases and nitroreductases (NTRs). Although nitroreductases have also been assigned to the EC 1.5 and 1.7 subclasses depending on their mechanism of action, most nitroreductases targeted by probes in Table 1 are of the EC 1.6 subclass. The characteristic feature of quinone oxidoreductases and nitroreductases is their dependence on NAD(P)H as an electron source.

Quinone oxidoreductases such as NAD(P)H:quinone oxidoreductase isozyme 1 (hNQO1) are upregulated in many tumors and constitute promising therapeutic targets.[30] hNQO1 regulates the degradation of p53, p73α, and p33 tumor suppressors in breast, lung, liver, stomach, and kidney tumors, among others.[30] Probes **3**, **6**, and **7** target hNQO1 via a quinone propionic acid motif, whose redox potential was tuned to quench the naphthalimide fluorophore by PET.[31−33] Upon two-electron reduction by hNQO1, the resultant hydroquinone undergoes lactonization spurred by the *gem*-dimethyl substituents, in a manner akin to the trimethyl lock moiety (cf. EC 3.1.1, probe **32**). In probes **3** and **6**, the lactonization directly restores fluorescence, whereas in probe **7**, an additional autoimmolative rearrangement step is necessary. Nonetheless, the hNQO1-mediated activation of probe **7** was found to be 2 orders of magnitude faster than that of **3** or **6**, largely because of steric factors. Probe **7** also benefits from reduced phototoxicity and background autofluorescence. As a result of the favorable toxicity profiles and enzymic response of the naphthalimide probes, rapid identification of hNQO1-positive cells was achieved with probe **7** in <10 min with positive to negative ratios of >500. More recently, a cyanine-based probe with a similar masking group strategy was applied to three-dimensional tumor spheroids and ovarian cancer mouse models.[34]

Similar to quinone oxidoreductases, two-electron nitroreductases are homodimers that employ NAD(P)H to reduce nitrogen-containing functional groups with aid from FMN as a cofactor. NTR activity is largely absent in most noncancerous human tissue but highly prevalent in bacteria, with *E. coli* and *Enterobacter cloacae* nitroreductases being of particular interest.[35,36] Interestingly, *E. cloacae* NTR was first isolated from bacteria that metabolize TNT and were discovered in a munitions factory.[35] Recent work with bacterial nitroreductases has focused on the rapid identification of pathogens, an application that benefits greatly from the low background and rapid response of fluorogenic probes. Probe **8** consists of a Cy5.5 fluorophore linked to an NTR-responsive nitroimidazole quencher.[11] As a result of its cationic lipophilic nature, probe **8** readily penetrates both Gram-positive and Gram-negative bacteria and undergoes NTR-responsive regeneration of fluorescence. Probe **8** was utilized to identify and distinguish between key antibacterial-resistant pathogens *E. faceium*, *S. aureus*, *K. pneumoniae*, *A. baumannii*, and *P. aeruginosa*.

Inspired by recent reports of NTR activity in hypoxic tumor cells, probes **2** and **9**−**14** were created to study hypoxia-dependent nitroreductase activity in cancerous cells.[37−43] Probes **2**, **9**, and **10** were highly selective for nitroreductase in the presence of other biologically relevant reducing agents and were used in the imaging of live A549, HCT116, and HeLa cells. Spatial differences in nitroreductase activity between different cellular compartments can be studied using targeted probes such as **12**, a cationic conjugated polymer that accumulates in the nucleus, or **11**, which contains a lysosome-targeting morpholine moiety. These probes are selective and highly responsive to nitroreductases, enable targeted imaging, and span several regions of the visible spectrum, enabling further studies of hypoxic tumor masses and other hypoxia-related diseases such as stroke and cardiac ischemia.

In consideration of the putative prokaryotic origin of mitochondria and nitroreductases, probe **15** was created to search for intramitochondrial NTR activity in normoxic cancer cells.[24] The cationic and lipophilic nature of probe **15** enabled selective mitochondrial accumulation in live A549 cells and a selective NTR response over other background reductases. Probe **15** revealed intramitochondrial nitroreductase activity that was attenuated by bacterial NTR inhibitors. This strategy was then expanded to prepare a prodrug version of Antimycin A for targeted release in mitochondria, which showed enhanced biological activity in WI38, BT474, and DU145 cells.

Unlike the nitroaromatic enzyme-reactive moieties in probes **8**−**15**, probe **16** incorporates an aryl azido group as a mask. Surprisingly, probe **16** was selective for CYP450 enzymes (EC 1.14) rather than the expected cytochrome P450 reductases.[44] This orthogonal response could be exploited for imaging and delivery applications. On the other hand, the effective reduction of probe **16** in several different cancer cell lines suggests instability of the aryl azido groups commonly used for proximity proteomics and photoaffinity labeling.[45]

DOI: 10.1021/acschembio.8b00371
ACS Chem. Biol. 2018, 13, 1810−1823

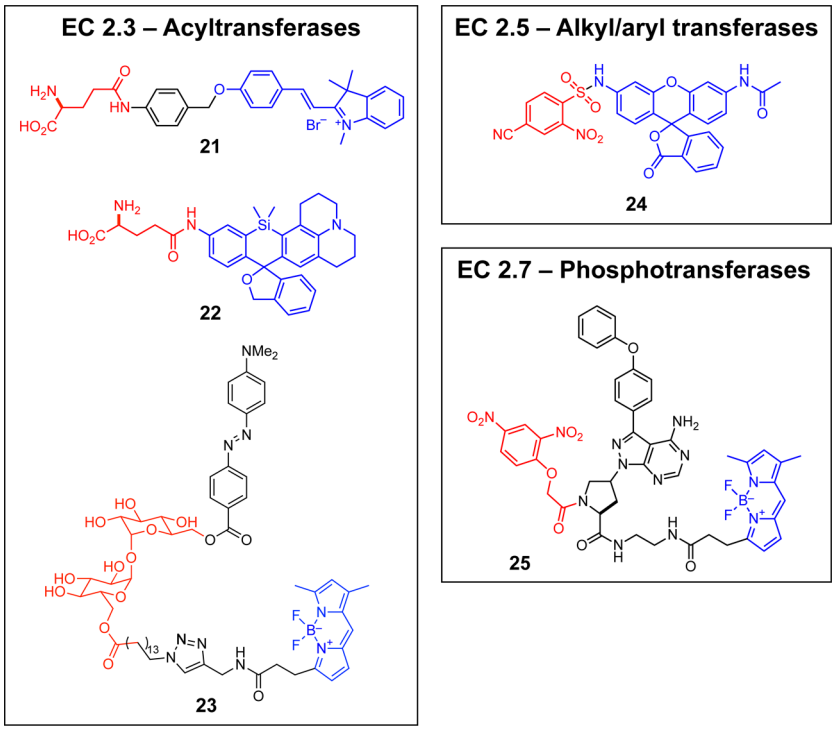

Figure 2. Structures of probes activated by transferase enzymes (EC 2). Enzyme-reactive moieties (red) and fluorophore scaffolds (blue) are highlighted.

Oxidoreductases Acting on Other Nitrogenous Compounds as Donors (EC 1.7). As an alternative to nitroreductase-responsive probes, probe **17** is responsive to *E. coli* azoreductase (EC 1.7.1.6), which reduces the azo group that links the rhodamine scaffold and the dimethylaniline autoimmolative linker.[46] Reduction of the azo group not only reverses PET quenching but also enables elimination of the parent rhodamine green dye. The azoreductase–probe pair can be used as an orthogonal reporter in any cell line amenable to transfection, including HeLa, A549, HEK293T, and NIH3T3. The slight susceptibility of the azo bond to nonspecific bioreduction under hypoxic conditions is, however, a potential limitation to the scope of applications.

Enzymes Acting on a Sulfur Group of Donors (EC 1.8). Thioredoxin reductase (TrxR) is a cornerstone of the thioredoxin pathway as the only known reductase of thioredoxin.[47] Similar to the nitroreductases described above, TrxR is a homodimer requiring NADPH and FMN cofactors. Probe **18** enables selective and rapid imaging of TrxR activity in live cells.[48] The selectivity arises from the five-membered cyclic disulfide attached to a naphthalimide fluorophore via a carbamate linker. Reduction by TxrR generates a thiolate that cleaves the carbamate linker to form a stable cyclic carbonothioate, releasing the naphthalimide fluorophore. Probe **18** resists nonspecific activation by reducing agents and closely related enzymes, as demonstrated by *in vitro* assays and live-cell imaging in Hep-G2 cells.

Enzymes Acting on Paired Donors, with Incorporation or Reduction of Molecular Oxygen (EC 1.14). Probe **19** enables the direct measurement of the activity of α-ketoglutarate-dependent dioxygenase alkB homologue 3 (ALKBH3), which is also known as prostate cancer antigen-1.[49] ALKBH3 demethylates 1-methyladenine in single-stranded DNA or RNA, and elevated levels of ALKBH3 are correlated with increased invasiveness and cell survival in cancer cells.[50] Probe **19** incorporates an electron-deficient 1-methyladenine quencher and adjacent pyrene fluorophores into a single strand of DNA. Enzymatic demethylation by ALKBH3 attenuates 1-methyladenine PET quenching, thus restoring pyrene fluorescence. Enzyme-optimized probe **19** possesses two pyrene nucleosides on the 3′ end of 1-methyladenine with symmetric poly(A) tails flanking both 3′ and 5′ ends for a total length of 10–12 nucleotides. The combination of length and positioning imbues probe **19** with steady state kinetic parameters that mirror those of native substrates and higher selectivity for ALKBH3 than for nine other homologues. As evidenced by flow cytometry and live-cell imaging with prostate cancer line PC3, probe **19** enables direct measurement of ALKBH3 activity in lieu of laborious immunohistochemistry or *in vitro* assays of enzymatic activity.

Another target of fluorogenic probes in subclass EC 1.14 is tyrosinase, an enzyme that converts phenols into *o*-quinones and limits the rate of melanin biosynthesis.[51] Although abnormal tyrosinase levels have been implicated in Parkinson's disease and vitiligo, detection and quantification of these enzymes are often complicated by cross-reactivity of probes with reactive oxygen species (ROS). To circumvent this limitation, near-infrared probe **20** incorporates a tyrosinase-responsive mask having an additional methylene group inserted between the hemicyanine fluorophore and aromatic ring, obviating ROS oxidation.[51] Elevated tyrosinase levels in murine melanoma B16 cells relative to HeLa cells were demonstrated by live-cell imaging with cell-permeable **20** and corroborated by an ELISA. Imaging zebrafish with probe **20** revealed previously unknown asymmetric distributions of tyrosinase between the yolk sac and tail.

DOI: 10.1021/acschembio.8b00371
ACS Chem. Biol. 2018, 13, 1810–1823

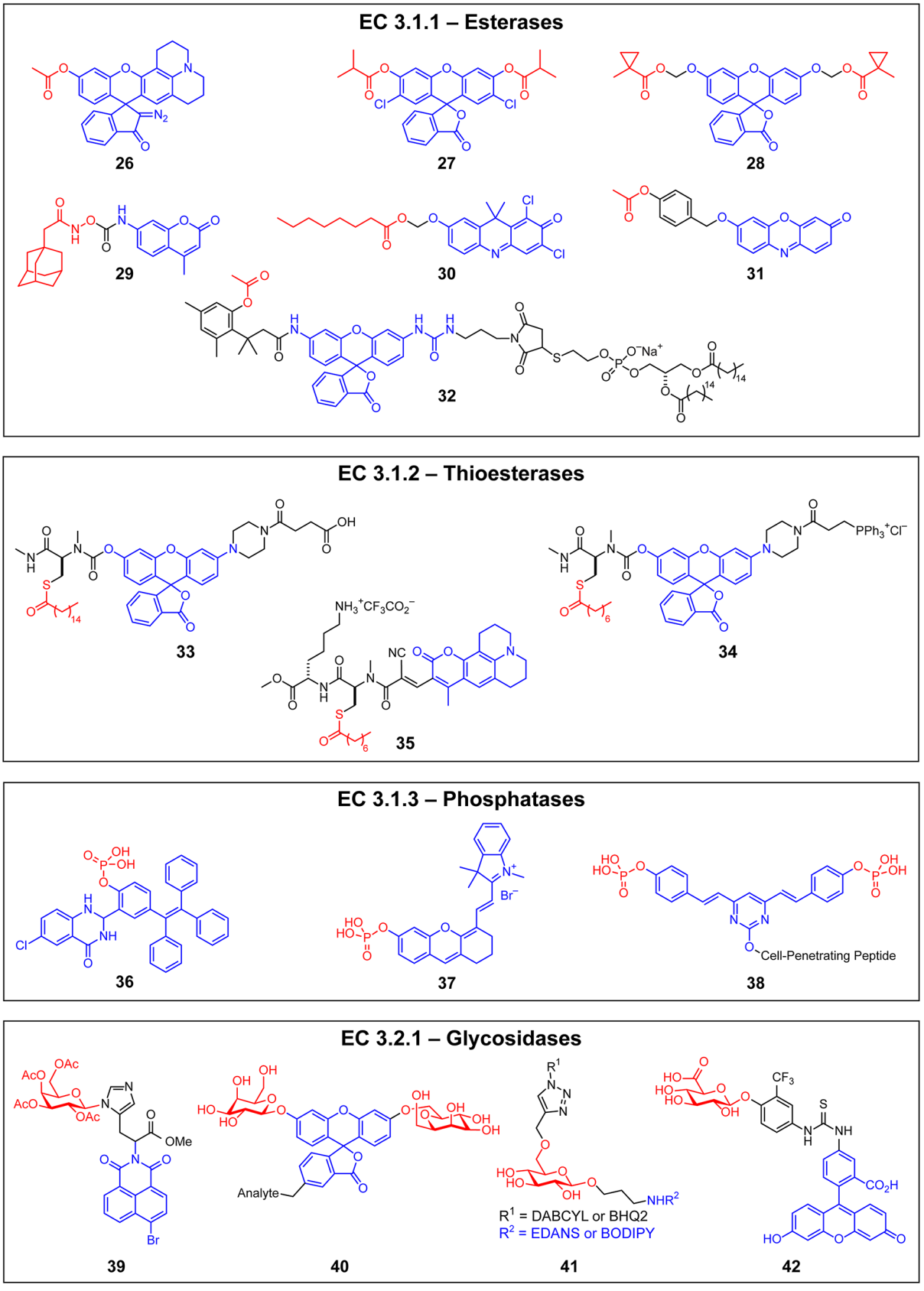

Figure 3. Structures of probes activated by hydrolases in classes EC 3.1 and EC 3.2. Enzyme-reactive moieties (red) and fluorophore scaffolds (blue) are highlighted.

DOI: 10.1021/acschembio.8b00371
ACS Chem. Biol. 2018, 13, 1810−1823

TRANSFERASES (EC 2)

Transferases facilitate the transfer of functional groups from donor to acceptor substrates and accommodate an extensive array of groups such as sulfuryl, phosphoryl, methyl, amino acyl, and acetyl groups (Figure 2).[28] Although transferases are essential to key biochemical pathways, fewer fluorogenic probes targeting transferases have been reported than those targeting the more frequently studied oxidoreductases (EC 1) or hydrolases (EC 3). This dichotomy is in part due to the difficulty of designing selective masking groups that can distinguish transferase activity from that of hydrolases and other enzymes. Indeed, early observations of transferase activity attributed the activity to a combination of hydrolases and other enzymes instead of a single transferase enzyme.[52] Recent probes that have achieved selective activation by transferases rely on transfer group mimetics (probes **21**–**23**),[53,54] specific acceptors (probe **24**),[55] or recognition moieties (probe **25**).[56]

Acyltransferases (EC 2.3). γ-Glutamyltransferase is one of approximately 32 aminoacyltransferases that act on amines to transfer peptide bonds.[28] γ-Glutamyltransferase-activated probes are of particular interest for oncologic surgeries because γ-glutamyltransferase is strongly expressed in a variety of cancers.[57] Fluorogenic probes for such intraoperative applications require rapid activation and low background to be effective. Probes **21** and **22** are activated by the enzyme-catalyzed hydrolysis of a glutamyl amide (which is a side reaction of γ-glutamyltransferase), releasing indocyanine or silarhodamine fluorophores. These probes, which share the same rapid-response masking group and minimize autofluorescence via red or near-infrared emission, have been used to image tumors in mouse intestines.

In mycobacteria, such as *M. tuberculosis*, acyltransferases play vital roles in cell-envelope biosynthesis.[58] FRET-quenched fluorogenic probe **23**[59] has been developed to study the spatiotemporal dynamics of mycolyltransferases that are essential for the construction of mycobacterial cell envelopes. Enzyme–probe specificity in probe **23** was achieved by using a substrate-mimetic linker between a BODIPY fluorophore and DABCYL quencher. Images of *M. smegmatis* obtained with this probe revealed that mycolyltransferase activity is asymmetric. Notably, fluorescence was generated by a hydrolytic side reaction catalyzed by mycolyltransferases, thereby leaving the cell envelope intact (cf. cytotoxic β-lactamase probes). The ability of this enzyme-activated probe to visualize mycobacteria selectively and with high sensitivity (>10^4-fold vs *E. coli* or *Bacillus subtilis*) suggests utility in the diagnosis of tuberculous.

Alkyl- or Aryltransferases (EC 2.5). Glutathione *S*-transferase (GST) is an important enzyme for the detoxification of xenobiotic substances through the transfer of glutathione for subsequent metabolic decomposition.[60] The structural variety of encountered xenobiotics exerts evolutionary pressure toward either a few enzymes with high substrate promiscuity or many substrate-specific enzymes. Ultimately, multiple isoforms of human GST evolved, with at least eight subclasses present in varied cellular locations, including the cytosol, mitochondria, and microsomes.[60] These defensive enzymes are also frequently commandeered by cancer cells to acquire drug resistance. GST catalyzes nucleophilic aromatic substitution of glutathione into probe **24** to form a Meisenheimer complex, which collapses to release the parent fluorophore.[55] Selectivity for the α and μ isoforms is achieved by tuning aryl substituents, and probe **24** was effective for imaging GST in HL60 cells.

Kinases (EC 2.7). Kinases are integral to signaling pathways and exhibit an extraordinary variety of substrates. The quantification and spatiotemporal tracking of a particular kinase activity have required multistep protocols involving the introduction of non-native proteins into cells.[61,62] As alternatives, probe **25**[56] and its analogues[63] have been developed for the single-step imaging of specific kinases. Probe **25** consists of three components, a Bruton's tyrosine kinase (Btk) inhibitor-based recognition moiety, a fluorophore–quencher pair, and a kinase-cleavable linker. A cysteine residue (Cys481) in the active site of Btk attaches covalently to the α-carbon of the amide linker in probe **25**, inducing elimination of the dinitrophenol quencher and enabling real-time imaging of Btk in live Namalwa cells. Because the kinase specificity of probe **25** is derived from the inhibitor mimic, this strategy is generally applicable to any kinase with accessible, selective small-molecule inhibitors.

HYDROLASES (EC 3)

Hydrolases, which catalyze the hydrolytic cleavage of chemical bonds, are preeminent targets of enzyme-activated fluorogenic probes. Early work with enzyme-activated probes was predominately on hydrolase-activated probes, which continue to be important tools for intracellular drug delivery,[64] imaging of dynamic cell processes,[20] and diagnostics and therapeutics.[65−67]

Esterases (EC 3.1.1). Esterases are particularly amenable to repurposing for drug delivery and diagnostic applications. Masking negatively charged carboxylic acids with esters is a proven technique for enhancing intracellular delivery of sensors, biomolecules,[68] and therapeutic agents.[64] Recent advances in esterase-activated probes include improvements in performance and utility (probes **26**–**28**) and new applications in therapeutics, pathogen detection, and cell physiology (probes **29**–**32**) (Figure 3).

Probe **26** is a dual-input probe for the super-resolution imaging of enzymatic activity. Many super-resolution microscopy techniques require photoactivatable probes, which is achieved with probe **26** by replacing the traditional xanthene lactone with a diazo moiety.[69] Because the esterase-reactive masking group is installed in a manner independent of the diazo moiety, this strategy can also be used to target other classes of enzymes in live-cell imaging. Probe **27** provides high stability, brightness, and photostability because of generally applicable electronic and steric optimization of the fluorophore and esterase-labile masking group.[70,71] Probe **28** along with exogenous pig liver esterase forms an enzyme–probe pair that is orthogonal to esterases in human cells. This pair enables an additional dimension of selectivity and demonstrates the feasibility of overlaying multiple enzymes catalyzing similar reactions in a single biological system while also preserving neatly discernible enzymatic responses.

In recent applications, esterase-activated fluorogenic probes **29** and **30** were shown to target bacterial enzymes relevant to botulism and tuberculosis. Probe **29** is a combination therapeutic and diagnostic agent, or "theranostic",[72] with a dual-purpose masking group that is also a potent inhibitor of botulinum neurotoxins.[23] A hydroxamate linker enables **29** to undergo esterase-catalyzed activation of the prodrug and fluorogenic probe after freely diffusing across the plasma membrane, with enhanced intracellular delivery and effective-

DOI: 10.1021/acschembio.8b00371
ACS Chem. Biol. 2018, 13, 1810−1823

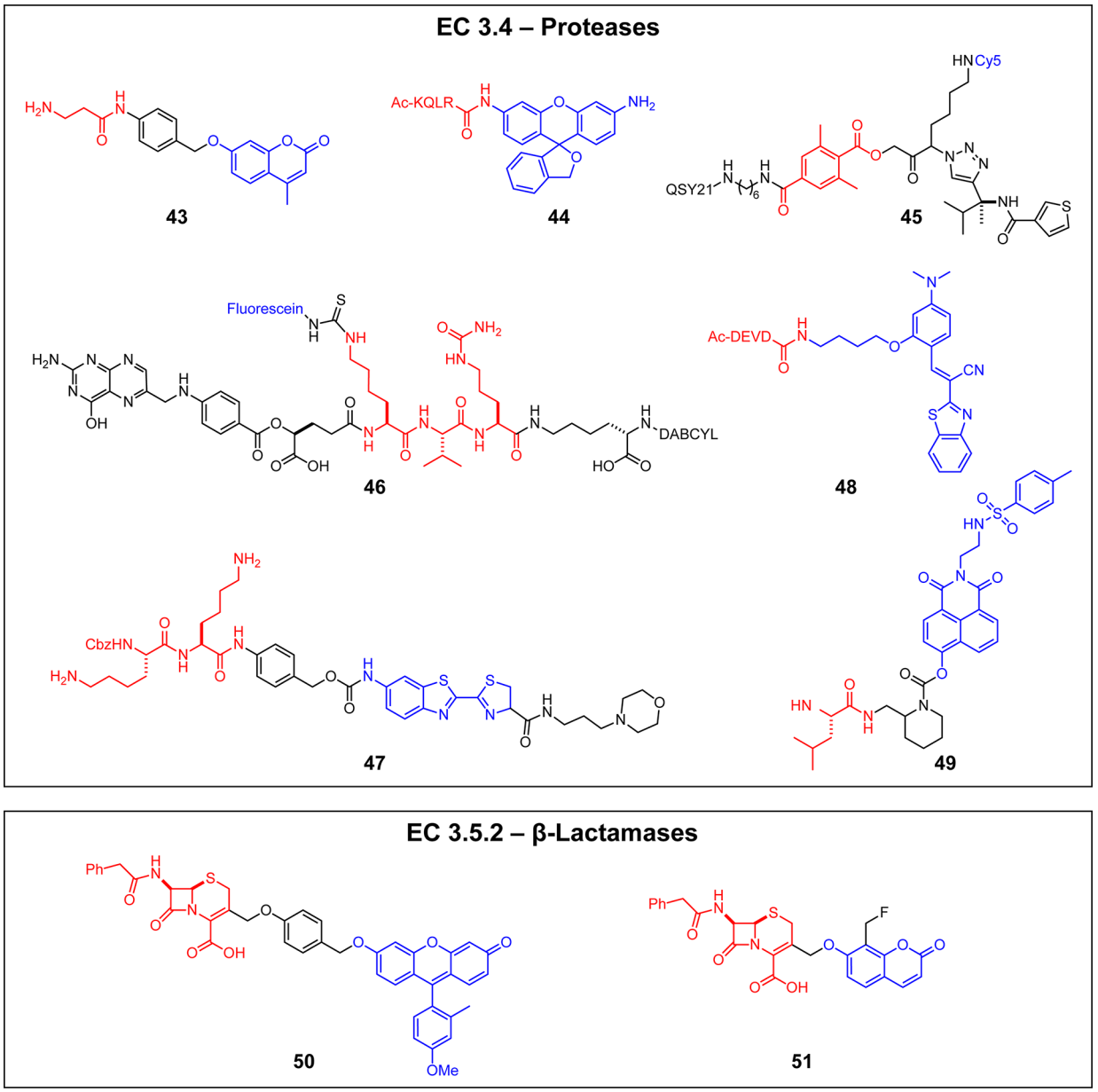

Figure 4. Structures of probes activated by hydrolases in classes EC 3.4 and EC 3.5. Enzyme-reactive moieties (red) and fluorophore scaffolds (blue) are highlighted.

ness in live neurons. Probe **30** is a far-red sensor with variable lipid tails for profiling bacterial esterase and lipase activities.[73] By testing samples with a battery of probes containing different lipid moieties, one can use a characteristic esterase fingerprint to distinguish *M. tuberculosis* from similar bacterial strains. In contrast to bacterial probes **29** and **30**, probes **31** and **32** function in human cells to provide refined spatiotemporal control and detailed physiological information. Probe **31** is one of a family of probes tuned to report esterase activity in the endoplasmic reticulum selectively, with potential for application as a drug release trigger.[74] Probe **32** contains a phosphatidylglycerol moiety, allowing it to embed in the outer surface of cells and monitor endocytic events.[20] The internalization of probe **32** allows intracellular esterases to unmask fluorescence, a feature that was used to demonstrate fundamental differences in rates of endocytosis in matched cancer and non-cancer cell lines.

Thioesterases (EC 3.1.2). The *S*-acylation of cysteine residues is a dynamic post-translational modification prevalent in mammalian cells. The degree of protein *S*-acylation is tuned by the careful balance between *S*-acyltransferases and thioesterases, which are themselves regulated by a variety of cell processes, including lipid signaling cascades, neuronal activation, and growth factor signaling.[75] Reversible *S*-palmitoylation is of particular interest given its association with disease and the importance of palmitoylation for proper protein location and function.[76]

Acyl-protein thioesterase 1 and 2 (APT1 and APT2, respectively) are depalmitoylases essential for the regulation of *S*-palmitoylation in the cytosol. Probes **33**−**35** target APT1 and APT2 via a substrate mimic that, upon activation, undergoes intramolecular cleavage of a carbamate to release coumarin or rhodol fluorophores.[77−79] The carboxylic acid in probe **33** increases the aqueous solubility, enabling inclusion of

DOI: 10.1021/acschembio.8b00371
ACS Chem. Biol. 2018, 13, 1810−1823

a native *S*-palmitoyl trigger substrate compared to the abbreviated *S*-octanoyl triggers in probes **34** and **35**.[79] Discovery of previously unknown mitochondrial depalmitoylase activity was accomplished by appending a triphenylphosphine moiety to yield mitochondrially targeted probe **34**.[77] In addition, imaging of live HEK293T cells with an APT1-preferential probe variant showed that APT1 is the primary enzyme responsible for mitochondrial depalmitoylation. To improve quantification of APT activity, ratiometric probe **35** was prepared from a substituted aminocoumarin and used to visualize cellular responses to lipid stress and APT activity in human colon organoids.[78] Probes **33**−**35** constitute a portfolio of tools for studying the spatiotemporal dynamics of APT1 and APT2 activity.

Phosphatases (EC 3.1.3). Minimizing background and deep-tissue imaging are common themes of probes **36**−**38**, which target alkaline phosphatases (ALP) or protein tyrosine phosphatases (PTP), enzymes that play key roles in disease pathogenesis and cell regulation.[80] ALP probe **36** was designed to detect secreted phosphatases, triggering excited state intramolecular proton transfer (ESIPT) fluorescence enhancement and irreversibly staining the surrounding area via fluorophore precipitation. Probe **36** was able to distinguish cells with different physiological profiles in heterogeneous tumor tissues.[81] In contrast to the sedimentary nature of probe **36**, near-infrared probe **37** was designed for dynamic imaging of ALP in live mice.[14] Probe **38**, which targets PTP, is a two-photon acyloxymethyl ketone probe conjugated to cell-penetrating peptides to facilitate organelle-specific detection at tissue depths of ≤100 μm.[82] Far-red PTP probe **1** provides reduced phototoxicity and background autofluorescence along with enhanced cellular uptake compared to those of existing PTP probes. Probe **1** was used to image PTP activity in HeLa cells and to identify *S. aureus* from a panel of similar human pathogens.[13]

Glycosidases (EC 3.2.1). Glycosidase-activated probes typically incorporate monosaccharides as masking groups or cleavable linkers for FRET quenching. Probes **39** and **40** are activated by β-galactosidase and are based on naphthalimide and xanthene scaffolds, respectively.[83,84] Two-photon excited probe **39** is designed to identify cell senescence in live SK-MEL-103 cells and xenograft tumor-imaging experiments.[84] Bioconjugable probe **40**, together with *E. coli* β-galactosidase installed in the cytosol, forms an enzyme−probe pair for quantification of the entry of the exogenous protein into the cytosol of HeLa cells.[83] Similar pairs with near-infrared emission profiles have been developed for general imaging applications in other cell lines.[85] Probe **41** detects lysosomal glucocerebrosidase activity, which is deficient in Gaucher's disease,[86] via cleavage of the glycosidic bond to release the parent fluorophore. The modularity of the linkers, quenchers, and fluorophores provides access to a variety of wavelengths for imaging fibroblasts. Probe **42** is similarly modular but instead employs masking groups activated by β-glucuronidase,[87] a promising enzyme for prodrug activation.[88,89] The linker between the masking group and near-infrared fluorophore contains a latent *o*-quinone methide electrophile that covalently binds the activated probe to the β-glucuronidase enzyme, a trapping motif also in β-lactamase probe **51** (EC 3.5.2). Trappable probe **42** has been used to visualize both subcutaneous and deep-tissue liver tumors in mice.

Proteases (EC 3.4). Proteases, enzymes that cleave peptide bonds, act with varying degrees of substrate discrimination. Targeting highly specific proteases with enzyme-activated fluorogenic probes can be achieved by incorporating peptides or peptide mimics as masking groups or linkers. Depending on the desired enzyme target, these protease recognition moieties can range from a single amino acid to >20 residues. Although activation mechanisms in protease-activated probes have been fairly constant, recent advances have enhanced probe performance, selectivity, and breadth of applications (Figure 4).

Probe **43** detects β-alanyl aminopeptidase activity in *P. aeruginosa*, a multi-drug-resistant pathogen commonly found in hospital-acquired infections.[90] The β-alanyl masking group of the probe was applied to resorufin, naphthalimide, and other fluorophore scaffolds to create panels of probes with clinical utility for identifying *P. aeruginosa* in culture.[91]

Probes **44**−**47** are designed for tumor visualization to improve diagnosis and intraoperative inspection during surgery. Probe **44** contains a single KQLR peptide masking group that is selectively cleaved by hepsin matriptase in prostate tumors.[92] By leveraging the pH-dependent fluorescence of the masked probe relative to that of the parent hydroxymethyl rhodamine, one can achieve high contrast ratios even using only a single masking group. The diagnostic utility of probe **44** was established broadly in live-cell and mouse imaging experiments. Probes **45**−**47** target cathepsins, a group of proteases activated in the acidic environment of lysosomes that have become a centerpiece of prodrug strategies.[93,94] Probe **45** is a non-peptide activity-based probe containing an electrophilic moiety that first selectively labels cathepsin S and then eliminates a quencher (QSY21), resulting in covalently labeling the enzyme with a fluorophore (Cy5).[95] Probe **45**, when deployed with nonspecific cathepsin-activated sister probes, has been instrumental for imaging syngeneic mammary tumors *in vivo* and profiling pathways of endolysosomal proteolysis in live dendritic cells. Probes **46** and **47** and others incorporate short peptides targeting cathepsin B and have been used for selective imaging of cathepsin B in a wide variety of cell lines (Table 1).[65,96] A discussion of protease-targeted activity-based probes and their clinical applications can be found elsewhere.[97−100]

Protease probes **48** and **49** rely on amino acid or peptide masking groups to target different proteases. Upon cleavage of the DEVD peptide in probe **48** by apoptotic protease caspase-3, the released monomer forms hydrophobic excimers with long-wavelength fluorescence.[101] Excimer formation spurs precipitation of aggregates, enabling live-cell imaging of location-specific caspase activity without the risk of fluorophore diffusion after cell apoptosis. Probe **49**, which targets endoplasmic reticulum (ER) aminopeptidase 1, is a two-photon excited fluorescent probe that undergoes a bicyclic urea cyclization to release an ER-targeted naphthalimide.[102] Selective enzymatic hydrolysis of the appropriate amide bond by the desired enzyme target, rather than nonspecific cleavage of thiourea and carbamate linkers in probes **46**, **47**, and **49**, was confirmed by the absence of an undesirable background signal upon incubation with nontarget proteases.

β-Lactamases (EC 3.5.2). Because of their clinical significance in antibiotic resistance, β-lactamases are frequent targets for fluorogenic probes in this class. With >890 β-lactamases having been identified to date, these cyclic amide hydrolases seriously challenge the efficacy of current antibiotics portfolios.[103] Advances in β-lactamase-activated probes focus

DOI: 10.1021/acschembio.8b00371
ACS Chem. Biol. 2018, 13, 1810−1823

primarily on improvements to the mechanism of activation and enzymatic specificity, enabling clinically crucial identification of different antibiotic-resistant bacteria. A challenge in the development of meaningful probes for β-lactamases is the intrinsic cytotoxicity of β-lactams, which can limit the usable concentration of these probes for live-cell imaging.

Probe **50** selectively targets BlaC, a β-lactamase overexpressed in *M. tuberculosis*.[66] Specificity was attained by tuning substituents to complement the substrate recognition loop in BlaC. As a result, probe **50** is 10^4-fold more responsive to BlaC than to homologous β-lactamases (e.g., TEM-1) and can identify *M. tuberculosis* in human sputum, though with a false-positive rate of 27%.

β-Lactamase generates a highly reactive Michael acceptor from probe **51**, comparable to the action of β-glucaronidase probe **42**.[67] The nascent electrophile forms covalent bonds with nucleophilic residues of β-lactamase before probe diffusion occurs, enabling spatiotemporal tracking of the enzyme. The utility of this approach was demonstrated in *E. coli* cells that produce β-lactamase.

FUTURE DIRECTIONS

Enzyme-activated fluorogenic probes are highly sensitive tools for biological imaging applications. Advances in probe design and application have expanded the toolkit for assessing enzymatic activity and have established generalizable methods for imaging in live-cell and *in vivo* model systems.

Future work will likely focus on two primary areas, enhanced specificity of enzyme activation and improved probe chemistries. The attainable spatiotemporal and physiological information for imaging experiments is related directly to the degree of enzyme specificity. Expanding the palette of single enzyme-specific probes (i.e., **24** and **45**) and isoform-specific probes (i.e., **4** and **5**) would provide higher-resolution information for identifying the location and function of a particular enzyme amidst the intracellular tapestry. Alternatively, new orthogonal enzyme−probe systems involving probes like **28** and **40** could be used to interrogate biological processes selectively while minimizing undesirable noise from endogenous enzymes. A logical extension of improved selectivity would be new theranostic agents such as probe **29**, which deliver targeted therapeutic agents and illuminate disease sites simultaneously.

Improved probe chemistries would enhance the photophysical performance of parent fluorophore scaffolds and improve enzymatic responses.[19] Tuning masking groups and enzyme recognition moieties, as demonstrated in probes **27** and **45**, could yield greater stability, reduced background, and enhanced activation kinetics. The incorporation of highly tunable[17] and multi-input[104,105] fluorophore scaffolds into new probes would facilitate sophisticated biological imaging and provide new insight into fundamental aspects of cell biology and physiology.

AUTHOR INFORMATION

Corresponding Author

*E-mail: rtraines@mit.edu.

ORCID

Ronald T. Raines: 0000-0001-7164-1719

Notes

The authors declare no competing financial interest.

ACKNOWLEDGMENTS

W.C. was supported by a National Science Foundation Graduate Research Fellowship. Work on fluorogenic probes in the Raines laboratory is supported by National Institutes of Health Grants R01 GM044783 and R01 CA073808.

REFERENCES

(1) Lakowicz, J. R. (2006) *Principles of Fluorescence Spectroscopy*, 3rd ed., Springer, New York.

(2) Chan, J., Dodani, S. C., and Chang, C. J. (2012) Reaction-based small-molecule fluorescent probes for chemoselective bioimaging. *Nat. Chem. 4*, 973−984.

(3) Grimm, J. B., Heckman, L. M., and Lavis, L. D. (2013) The chemistry of small-molecule fluorogenic probes. *Prog. Mol. Biol. Transl. 113*, 1−34.

(4) Nadler, A., and Schultz, C. (2013) The power of fluorogenic probes. *Angew. Chem., Int. Ed. 52*, 2408−2410.

(5) Rotman, B. (1961) Measurement of activity of single molecules of β-D-galactosidase. *Proc. Natl. Acad. Sci. U. S. A. 47*, 1981−1991.

(6) Rotman, B., Zderic, J. A., and Edelstein, M. (1963) Fluorogenic substrates for β-D-galactosidases and phosphatases derived from fluorescein (3,6-dihydroxyfluoran) and its monomethyl ether. *Proc. Natl. Acad. Sci. U. S. A. 50*, 1−6.

(7) Kramer, D. N., and Guilbault, G. G. (1963) A substrate for the fluorometric determination of lipase activity. *Anal. Chem. 35*, 588−589.

(8) Guilbault, G. G., and Kramer, D. N. (1965) Resorufin butyrate and indoxyl acetate as fluorogenic substrates for cholinesterase. *Anal. Chem. 37*, 120−123.

(9) Rotman, B., and Papermaster, B. W. (1966) Membrane properties of living mammalian cells as studied by enzymatic hydrolysis of fluorogenic esters. *Proc. Natl. Acad. Sci. U. S. A. 55*, 134−141.

(10) Jones, K. H., and Senft, J. A. (1985) An improved method to determine cell viability by simultaneous staining with fluorescein diacetate−propidium iodide. *J. Histochem. Cytochem. 33*, 77−79.

(11) Xu, S., Wang, Q., Zhang, Q., Zhang, L., Zuo, L., Jiang, J.-D., and Hu, H.-Y. (2017) Real time detection of ESKAPE pathogens by a nitroreductase-triggered fluorescence turn-on probe. *Chem. Commun. 53*, 11177−11180.

(12) Coutlee, F., Viscidi, R. P., and Yolken, R. H. (1989) Comparison of colorimetric, fluorescent, and enzymatic amplification substrate systems in an enzyme-immunoassay for detection of DNA−RNA hybrids. *J. Clin. Microbiol. 27*, 1002−1007.

(13) Biswas, S., McCullough, B. S., Ma, E. S., LaJoie, D., Russell, C. W., Garrett Brown, D., Round, J. L., Ullman, K. S., Mulvey, M. A., and Barrios, A. M. (2017) Dual colorimetric and fluorogenic probes for visualizing tyrosine phosphatase activity. *Chem. Commun. 53*, 2233−2236.

(14) Tan, Y., Zhang, L., Man, K. H., Peltier, R., Chen, G., Zhang, H., Zhou, L., Wang, F., Ho, D., Yao, S. Q., Hu, Y., and Sun, H. (2017) Reaction-based off−on near-infrared fluorescent probe for imaging alkaline phosphatase activity in living cells and mice. *ACS Appl. Mater. Interfaces 9*, 6796−6803.

(15) Li, L., Zhang, C.-W., Chen, G. Y. J., Zhu, B., Chai, C., Xu, Q.-H., Tan, E.-K., Zhu, Q., Lim, K.-L., and Yao, S. Q. (2014) A sensitive two-photon probe to selectively detect monoamine oxidase B activity in Parkinson's disease models. *Nat. Commun. 5*, 3276.

(16) Zheng, Q., and Lavis, L. D. (2017) Development of photostable fluorophores for molecular imaging. *Curr. Opin. Chem. Biol. 39*, 32−38.

(17) Grimm, J. B., Muthusamy, A. K., Liang, Y., Brown, T. A., Lemon, W. C., Patel, R., Lu, R., Macklin, J. J., Keller, P. J., Ji, N., and Lavis, L. D. (2017) A general method to fine-tune fluorophores for live-cell and *in vivo* imaging. *Nat. Methods 14*, 987−994.

(18) Lavis, L. D., and Raines, R. T. (2008) Bright ideas for chemical biology. *ACS Chem. Biol. 3*, 142−155.

DOI: 10.1021/acschembio.8b00371
ACS Chem. Biol. 2018, 13, 1810−1823

(19) Lavis, L. D., and Raines, R. T. (2014) Bright building blocks for chemical biology. *ACS Chem. Biol. 9*, 855−866.
(20) Levine, M. N., Hoang, T. T., and Raines, R. T. (2013) Fluorogenic probe for constitutive cellular endocytosis. *Chem. Biol. 20*, 614−618.
(21) Ellis, R. J. (2001) Macromolecular crowding: Obvious but underappreciated. *Trends Biochem. Sci. 26*, 597−604.
(22) Minton, A. P. (2001) The influence of macromolecular crowding and macromolecular confinement on biochemical reactions in physiological media. *J. Biol. Chem. 276*, 10577−10580.
(23) Šilhár, P., Eubanks, L. M., Seki, H., Pellett, S., Javor, S., Tepp, W. H., Johnson, E. A., and Janda, K. D. (2013) Targeting botulinum A cellular toxicity: A prodrug approach. *J. Med. Chem. 56*, 7870−7879.
(24) Chevalier, A., Zhang, Y., Khdour, O. M., Kaye, J. B., and Hecht, S. M. (2016) Mitochondrial nitroreductase activity enables selective imaging and therapeutic targeting. *J. Am. Chem. Soc. 138*, 12009−12012.
(25) Levine, M. N., and Raines, R. T. (2012) Trimethyl lock: A trigger for molecular release in chemistry, biology, and pharmacology. *Chem. Sci. 3*, 2412−2420.
(26) Wu, X., Shi, W., Li, X., and Ma, H. (2017) A strategy for specific fluorescence imaging of monoamine oxidase A in living cells. *Angew. Chem., Int. Ed. 56*, 15319−15323.
(27) Rokita, S. E., Ed. (2009) *Quinone Methides*, John Wiley & Sons, Hoboken, NJ.
(28) Webb, E. C., Ed. (1992) *Enzyme Nomenclature 1992: Recommendations of the Nomenclature Committee of the International Union of Biochemistry and Molecular Biology on the Nomenclature and Classification of Enzymes*, Academic Press, San Diego.
(29) Shih, J. C., Chen, K., and Ridd, M. J. (1999) Monoamine oxidase: From genes to behavior. *Annu. Rev. Neurosci. 22*, 197−217.
(30) Ross, D., Kepa, J. K., Winski, S. L., Beall, H. D., Anwar, A., and Siegel, D. (2000) NAD(P)H:quinone oxidoreductase 1 (NQO1): Chemoprotection, bioactivation, gene regulation and genetic polymorphisms. *Chem.-Biol. Interact. 129*, 77−97.
(31) Silvers, W. C., Prasai, B., Burk, D. H., Brown, M. L., and McCarley, R. L. (2013) Profluorogenic reductase substrate for rapid, selective, and sensitive visualization and detection of human cancer cells that overexpress NQO1. *J. Am. Chem. Soc. 135*, 309−314.
(32) Hettiarachchi, S. U., Prasai, B., and McCarley, R. L. (2014) Detection and cellular imaging of human cancer enzyme using a turn-on, wavelength-shiftable, self-immolative profluorophore. *J. Am. Chem. Soc. 136*, 7575−7578.
(33) Prasai, B., Silvers, W. C., and McCarley, R. L. (2015) Oxidoreductase-facilitated visualization and detection of human cancer cells. *Anal. Chem. 87*, 6411−6418.
(34) Shen, Z., Prasai, B., Nakamura, Y., Kobayashi, H., Jackson, M. S., and McCarley, R. L. (2017) A near-infrared, wavelength-shiftable, turn-on fluorescent probe for the detection and imaging of cancer tumor cells. *ACS Chem. Biol. 12*, 1121−1132.
(35) Bryant, C., and DeLuca, M. (1991) Purification and characterization of an oxygen-insensitive NAD(P)H nitroreductase from *Enterobacter cloacae*. *J. Biol. Chem. 266*, 4119−4125.
(36) Williams, E. M., Little, R. F., Mowday, A. M., Rich, M. H., Chan-Hyams, J. V., Copp, J. N., Smaill, J. B., Patterson, A. V., and Ackerley, D. F. (2015) Nitroreductase gene-directed enzyme prodrug therapy: Insights and advances toward clinical utility. *Biochem. J. 471*, 131−153.
(37) Su, J., Guise, C. P., and Wilson, W. R. (2013) FSL-61 is a 6-nitroquinolone fluorogenic probe for one-electron reductases in hypoxic cells. *Biochem. J. 452*, 79−86.
(38) Li, Z., Li, X., Gao, X., Zhang, Y., Shi, W., and Ma, H. (2013) Nitroreductase detection and hypoxic tumor cell imaging by a designed sensitive and selective fluorescent probe, 7-[(5-nitrofuran-2-yl)methoxy]-3*H*-phenoxazin-3-one. *Anal. Chem. 85*, 3926−3932.
(39) Zhang, J., Liu, H.-W., Hu, X.-X., Li, J., Liang, L.-H., Zhang, X.-B., and Tan, W. (2015) Efficient two-photon fluorescent probe for nitroreductase detection and hypoxia imaging in tumor cells and tissues. *Anal. Chem. 87*, 11832−11839.
(40) Zhou, J., Shi, W., Li, L.-H., Gong, Q.-Y., Wu, X.-F., Li, X.-H., and Ma, H.-M. (2016) A lysosome-targeting fluorescence off−on probe for imaging of nitroreductase and hypoxia in live cells. *Chem. - Asian J. 11*, 2719−2724.
(41) Kim, T.-I., Kim, H., Choi, Y., and Kim, Y. (2017) *meso*-Ester BODIPYs for the imaging of hypoxia in tumor cells. *Sens. Actuators, B 249*, 229−234.
(42) Zhang, X., Zhao, Q., Li, Y., Duan, X., and Tang, Y. (2017) Multifunctional probe based on cationic conjugated polymers for nitroreductase-related analysis: Sensing, hypoxia diagnosis, and imaging. *Anal. Chem. 89*, 5503−5510.
(43) Jin, C., Zhang, Q., and Lu, W. (2017) Selective turn-on near-infrared fluorescence probe for hypoxic tumor cell imaging. *RSC Adv. 7*, 18217−18223.
(44) O'Connor, L. J., Mistry, I. N., Collins, S. L., Folkes, L. K., Brown, G., Conway, S. J., and Hammond, E. M. (2017) CYP450 enzymes effect oxygen-dependent reduction of azide-based fluorogenic dyes. *ACS Cent. Sci. 3*, 20−30.
(45) Pham, N. D., Parker, R. B., and Kohler, J. J. (2013) Photocrosslinking approaches to interactome mapping. *Curr. Opin. Chem. Biol. 17*, 90−101.
(46) Shin, N., Hanaoka, K., Piao, W., Miyakawa, T., Fujisawa, T., Takeuchi, S., Takahashi, S., Komatsu, T., Ueno, T., Terai, T., Tahara, T., Tanokura, M., Nagano, T., and Urano, Y. (2017) Development of an azoreductase-based reporter system with synthetic fluorogenic substrates. *ACS Chem. Biol. 12*, 558−563.
(47) Arnér, E. S. J., and Holmgren, A. (2000) Physiological functions of thioredoxin and thioredoxin reductase. *Eur. J. Biochem. 267*, 6102−6109.
(48) Zhang, L., Duan, D., Liu, Y., Ge, C., Cui, X., Sun, J., and Fang, J. (2014) Highly selective off−on fluorescent probe for imaging thioredoxin reductase in living cells. *J. Am. Chem. Soc. 136*, 226−233.
(49) Beharry, A. A., Lacoste, S., O'Connor, T. R., and Kool, E. T. (2016) Fluorescence monitoring of the oxidative repair of DNA alkylation damage by ALKBH3, a prostate cancer marker. *J. Am. Chem. Soc. 138*, 3647−3650.
(50) Camps, M., and Eichman, B. F. (2011) Unraveling a connection between DNA demethylation repair and cancer. *Mol. Cell 44*, 343−344.
(51) Wu, X., Li, L., Shi, W., Gong, Q., and Ma, H. (2016) Near-infrared fluorescent probe with new recognition moiety for specific detection of tyrosinase activity: Design, synthesis, and application in living cells and zebrafish. *Angew. Chem., Int. Ed. 55*, 14728−14732.
(52) Morton, R. K. (1953) Transferase activity of hydrolytic enzymes. *Nature 172*, 65−68.
(53) Park, S., Lim, S.-Y., Bae, S. M., Kim, S.-Y., Myung, S.-J., and Kim, H.-J. (2016) Indocyanine-based activatable fluorescence turn-on probe for γ-glutamyltranspeptidase and its application to the mouse model of colon cancer. *ACS Sens. 1*, 579−583.
(54) Iwatate, R. J., Kamiya, M., Umezawa, K., Kashima, H., Nakadate, M., Kojima, R., and Urano, Y. (2018) Silicon rhodamine-based near-infrared fluorescence probe for γ-glutamyltransferase. *Bioconjugate Chem. 29*, 241−244.
(55) Shibata, A., Nakano, Y., Ito, M., Araki, M., Zhang, J., Yoshida, Y., Shuto, S., Mannervik, B., Mogenstern, R., Ito, Y., and Abe, H. (2013) Fluorogenic probes using 4-substituted-2-nitrobenzenesulfonyl derivatives as caging groups for the analysis of human glutathione transferase catalyzed reactions. *Analyst 138*, 7326−7330.
(56) Zhang, Q., Liu, H., and Pan, Z. (2014) A general approach for the development of fluorogenic probes suitable for no-wash imaging of kinases in live cells. *Chem. Commun. 50*, 15319−15322.
(57) Corti, A., Franzini, M., Paolicchi, A., and Pompella, A. (2010) Gamma-glutamyltransferase of cancer cells at the cossroads of tumor progression, drug resistance and drug targeting. *Anticancer Res. 30*, 1169−1181.
(58) Röttig, A., and Steinbüchel, A. (2013) Acyltransferases in bacteria. *Microbiol. Mol. Biol. Rev. 77*, 277−321.

DOI: 10.1021/acschembio.8b00371
ACS Chem. Biol. 2018, 13, 1810−1823

(59) Hodges, H. L., Brown, R. A., Crooks, J. A., Weibel, D. B., and Kiessling, L. L. (2018) Fluorogenic probe for imaging mycobacterial growth and division. *Proc. Natl. Acad. Sci. U. S. A. 115*, 5271−5276.
(60) Salinas, A. E., and Wong, M. G. (1999) Glutathione *S*-transferases—A review. *Curr. Med. Chem. 6*, 279−309.
(61) Ng, T., Squire, A., Hansra, G., Bornancin, F., Prevostel, C., Hanby, A., Harris, W., Barnes, D., Schmidt, S., Mellor, H., Bastiaens, P. I. H., and Parker, P. J. (1999) Imaging protein kinase Cα activation in cells. *Science 283*, 2085−2089.
(62) Zhang, L., Lee, K. C., Bhojani, M. S., Khan, A. P., Shilman, A., Holland, E. C., Ross, B. D., and Rehemtulla, A. (2007) Molecular imaging of Akt kinase activity. *Nat. Med. 13*, 1114−1119.
(63) Zuo, Y., Shi, Y., Li, X., Teng, Y., and Pan, Z. (2015) A novel 2,5-diaminopyrimidine-based affinity probe for Bruton's tyrosine kinase. *Sci. Rep. 5*, 16136.
(64) Testa, B., and Mayer, J. M. (2003) *Hydrolysis in Drug and Prodrug Metabolism: Chemistry, Biochemistry, and Enzymology*, Verlag Helvetica Chimica Acta, Zürich.
(65) Tian, R., Li, M., Wang, J., Yu, M., Kong, X., Feng, Y., Chen, Z., Li, Y., Huang, W., Wu, W., and Hong, Z. (2014) An intracellularly activatable, fluorogenic probe for cancer imaging. *Org. Biomol. Chem. 12*, 5365−5374.
(66) Cheng, Y., Xie, H., Sule, P., Hassounah, H., Graviss, E. A., Kong, Y., Cirillo, J. D., and Rao, J. (2014) Fluorogenic probes with substitutions at the 2 and 7 positions of cephalosporin are highly BlaC-specific for rapid *Mycobacterium tuberculosis* detection. *Angew. Chem., Int. Ed. 53*, 9360−9364.
(67) Mao, W., Xia, L., Wang, Y., and Xie, H. (2016) A self-immobilizing and fluorogenic probe for β-lactamase detection. *Chem. - Asian J. 11*, 3493−3497.
(68) Mix, K. A., Lomax, J. E., and Raines, R. T. (2017) Cytosolic delivery of proteins by bioreversible esterification. *J. Am. Chem. Soc. 139*, 14396−14398.
(69) Halabi, E. A., Thiel, Z., Trapp, N., Pinotsi, D., and Rivera-Fuentes, P. (2017) A photoactivatable probe for super-resolution imaging of enzymatic activity in live cells. *J. Am. Chem. Soc. 139*, 13200−13207.
(70) Chyan, W., Kilgore, H. R., Gold, B., and Raines, R. T. (2017) Electronic and steric optimization of fluorogenic probes for biomolecular imaging. *J. Org. Chem. 82*, 4297−4304.
(71) Chyan, W., Kilgore, H. R., and Raines, R. T. (2018) Cytosolic uptake of large monofunctionalized dextrans. *Bioconjugate Chem. 29*, 1942−1949.
(72) Thanou, M., Ed. (2018) *Theranostics and Image Guided Drug Delivery*, The Royal Society of Chemistry, London.
(73) Tallman, K. R., Levine, S. R., and Beatty, K. E. (2016) Profiling esterases in *Mycobacterium tuberculosis* using far-red fluorogenic substrates. *ACS Chem. Biol. 11*, 1810−1815.
(74) Hakamata, W., Tamura, S., Hirano, T., and Nishio, T. (2014) Multicolor imaging of endoplasmic reticulum-located esterase as a prodrug activation enzyme. *ACS Med. Chem. Lett. 5*, 321−325.
(75) Zeidman, R., Jackson, C. S., and Magee, A. I. (2009) Protein acyl thioesterases (review). *Mol. Membr. Biol. 26*, 32−41.
(76) Yeste-Velasco, M., Linder, M. E., and Lu, Y.-J. (2015) Protein *S*-palmitoylation and cancer. *Biochim. Biophys. Acta, Rev. Cancer 1856*, 107−120.
(77) Kathayat, R., Cao, Y., Elvira, P. D., Sandoz, P. A., Zaballa, M.-E., Springer, M. Z., Drake, L. E., Macleod, K. F., van der Goot, F. G., and Dickinson, B. C. (2018) Active and dynamic mitochondrial *S*-depalmitoylation revealed by targeted fluorescent probes. *Nat. Commun. 9*, 334.
(78) Beck, M. W., Kathayat, R. S., Cham, C. M., Chang, E. B., and Dickinson, B. C. (2017) Michael addition-based probes for ratiometric fluorescence imaging of protein *S*-depalmitoylases in live cells and tissues. *Chem. Sci. 8*, 7588−7592.
(79) Qiu, T., Kathayat, R. S., Cao, U., Beck, M. W., and Dickinson, B. C. (2018) A fluorescent probe with improved water solubility permits the analysis of protein *S*-depalmitoylation activity in live cells. *Biochemistry 57*, 221−225.
(80) Coleman, J. E. (1992) Structure and mechanism of alkaline-phosphatase. *Annu. Rev. Biophys. Biomol. Struct. 21*, 441−483.
(81) Liu, H.-W., Li, K., Hu, X.-X., Zhu, L., Rong, Q., Liu, Y., Zhang, X.-B., Hasserodt, J., Qu, F.-L., and Tan, W. (2017) *In situ* localization of enzyme activity in live cells by a molecular probe releasing a precipitating fluorochrome. *Angew. Chem., Int. Ed. 56*, 11788−11792.
(82) Li, L., Ge, J., Wu, H., Xu, Q.-H., and Yao, S. Q. (2012) Organelle-specific detection of phosphatase activities with two-photon fluorogenic probes in cells and tissues. *J. Am. Chem. Soc. 134*, 12157−12167.
(83) Chao, T.-Y., and Raines, R. T. (2013) Fluorogenic label to quantify the cytosolic delivery of macromolecules. *Mol. BioSyst. 9*, 339−342.
(84) Lozano-Torres, B., Galiana, I., Rovira, M., Garrido, E., Chaib, S., Bernardos, A., Muñoz-Espín, D., Serrano, M., Martínez-Máñez, R., and Sancenón, F. (2017) An OFF−ON two-photon fluorescent probe for tracking cell senescence *in vivo*. *J. Am. Chem. Soc. 139*, 8808−8811.
(85) Han, J., Han, M. S., and Tung, C.-H. (2013) A fluorogenic probe for β-galactosidase activity imaging in living cells. *Mol. BioSyst. 9*, 3001−3008.
(86) Yadav, A. K., Shen, D. L., Shan, X., He, X., Kermode, A. R., and Vocadlo, D. J. (2015) Fluorescence-quenched substrates for live cell imaging of human glucocerebrosidase activity. *J. Am. Chem. Soc. 137*, 1181−1189.
(87) Cheng, T.-C., Roffler, S. R., Tzou, S.-C., Chuang, K.-H., Su, Y.-C., Chuang, C.-H., Kao, C.-H., Chen, C.-S., Harn, I.-H., Liu, K.-Y., Cheng, T.-L., and Leu, Y.-L. (2012) An activity-based near-infrared glucuronide trapping probe for imaging β-glucuronidase expression in deep tissues. *J. Am. Chem. Soc. 134*, 3103−3110.
(88) de Graaf, M., Boven, E., Scheeren, H. W., Haisma, H. J., and Pinedo, H. M. (2002) Beta-glucuronidase−mediated drug release. *Curr. Pharm. Des. 8*, 1391−1403.
(89) Burke, P. J., Hamilton, J. Z., Jeffrey, S. C., Hunter, J. H., Doronina, S. V., Okeley, N. M., Miyamoto, J. B., Anderson, M. E., Stone, I. J., Ulrich, M. L., Simmons, J. K., McKinney, E. E., Senter, P. D., and Lyon, R. P. (2017) Optimization of a PEGylated glucuronide-monomethylauristatin E linker for antibody−drug conjugates. *Mol. Cancer Ther. 16*, 116−123.
(90) Váradi, L., Hibbs, D. E., Orenga, S., Babolat, M., Perry, J. D., and Groundwater, P. W. (2016) β-Alanyl aminopeptidase-activated fluorogenic probes for the rapid identification of *Pseudomonas aeruginosa* in clinical samples. *RSC Adv. 6*, 58884−58889.
(91) Luo, J. L., Jin, T., Váradi, L., Perry, J. D., Hibbs, D. E., and Groundwater, P. W. (2016) Evaluation of fluorogenic amino-naphthalenesulfonamides and 6-hydrazinobenz[de]isoquinoline-1,3-diones for the detection of bacteria. *Dyes Pigm. 125*, 15−26.
(92) Yogo, T., Umezawa, K., Kamiya, M., Hino, R., and Urano, Y. (2017) Development of an activatable fluorescent probe for prostate cancer imaging. *Bioconjugate Chem. 28*, 2069−2076.
(93) Dubowchik, G. M., Firestone, R. A., Willner, D., Hofstead, S. J., Trail, P. A., Lasch, S. J., Henderson, A. J., Jure, M., Mosure, K. W., and Knipe, J. O. (1998) Peptide linkers for selective intralysosomal release of anticancer drugs from monoclonal antibody conjugates. In *Peptides 1996: Proceedings of the Twenty-Fourth European Peptide Symposium* (Ramage, R., and Epton, R., Eds.) pp 347−348, Mayflower Scientific, Kingswinford, U.K.
(94) Doronina, S. O., Toki, B. E., Torgov, M. Y., Mendelsohn, B. A., Cerveny, C. G., Chace, D. F., DeBlanc, R. L., Gearing, R. P., Bovee, T. D., Siegall, C. B., Francisco, J. A., Wahl, A. F., Meyer, D. L., and Senter, P. D. (2003) Development of potent monoclonal antibody auristatin conjugates for cancer therapy. *Nat. Biotechnol. 21*, 778−784.
(95) Oresic Bender, K., Ofori, L., van der Linden, W. A., Mock, E. D., Datta, G. K., Chowdhury, S., Li, H., Segal, E., Sanchez Lopez, M., Ellman, J. A., Figdor, C. G., Bogyo, M., and Verdoes, M. (2015) Design of a highly selective quenched activity-based probe and its application in dual color imaging studies of cathepsin S activity localization. *J. Am. Chem. Soc. 137*, 4771−4777.

DOI: 10.1021/acschembio.8b00371
ACS Chem. Biol. 2018, 13, 1810−1823

(96) Wang, Y., Li, J., Feng, L., Yu, J., Zhang, Y., Ye, D., and Chen, H.-Y. (2016) Lysosome-targeting fluorogenic probe for cathepsin B imaging in living cells. *Anal. Chem. 88*, 12403−12410.
(97) Verdoes, M., Oresic Bender, K., Segal, E., van der Linden, W. A., Syed, S., Withana, N. P., Sanman, L. E., and Bogyo, M. (2013) Improved quenched fluorescent probe for imaging of cysteine cathepsin activity. *J. Am. Chem. Soc. 135*, 14726−14730.
(98) Sanman, L. E., and Bogyo, M. (2014) Activity-based profiling of proteases. *Annu. Rev. Biochem. 83*, 249−273.
(99) Ofori, L. O., Withana, N. P., Prestwood, T. R., Verdoes, M., Brady, J. J., Winslow, M. M., Sorger, J., and Bogyo, M. (2015) Design of protease activated optical contrast agents that exploit a latent lysosomotropic effect for use in fluorescence-guided surgery. *ACS Chem. Biol. 10*, 1977−1988.
(100) Withana, N. P., Ma, X., McGuire, H. M., Verdoes, M., van der Linden, W. A., Ofori, L. O., Zhang, R., Li, H., Sanman, L. E., Wei, K., Yao, S., Wu, P., Li, F., Huang, H., Xu, Z., Wolters, P. J., Rosen, G. D., Collard, H. R., Zhu, Z., Cheng, Z., and Bogyo, M. (2016) Non-invasive imaging of idiopathic pulmonary fibrosis using cathepsin protease probes. *Sci. Rep. 6*, 19755.
(101) Kim, T.-I., Jin, H., Bae, J., and Kim, Y. (2017) Excimer emission-based fluorescent probe targeting caspase-3. *Anal. Chem. 89*, 10565−10569.
(102) Xu, S., Liu, H.-W., Hu, X.-X., Huan, S.-Y., Zhang, J., Liu, Y.-C., Yuan, L., Qu, F.-L., Zhang, X.-B., and Tan, W. (2017) Visualization of endoplasmic reticulum aminopeptidase 1 under different redox conditions with a two-photon fluorescent probe. *Anal. Chem. 89*, 7641−7648.
(103) Bush, K. (2010) Bench-to-bedside review: The role of β-lactamases in antibiotic-resistant Gram-negative infections. *Crit. Care 14*, 224.
(104) Grimm, J. B., Gruber, T. D., Ortiz, G., Brown, T. A., and Lavis, L. D. (2016) Virginia Orange: A versatile, red-shifted fluorescein scaffold for single- and dual-input fluorogenic probes. *Bioconjugate Chem. 27*, 474−480.
(105) Gonçalves, C. C. S., da Costa, B. Z., Lima, M. L. S. O., Fiorito, G. F., Ruiz, A. L. T. G., de Oliveira, S. B. P., Barbosa, G. O., de Carvalho, H. F., and Marsaioli, A. J. (2016) Enzymatic profiling in prostate and breast cancer cells: Phosphate hydrolysis and alcohol oxidation. *Tetrahedron 72*, 7235−7240.

DOI: 10.1021/acschembio.8b00371
ACS Chem. Biol. 2018, 13, 1810−1823